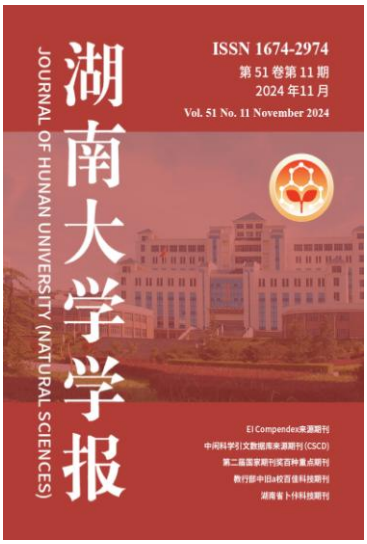

Journal of Hunan University

(Natural Sciences)

Vol. 51 No. 11

November 2024

Available online at

http://jonuns.com/index.php/journal/index

Open Access Article

https://doi.org/10.55463/issn.1674-2974.51.11.3

Optimization of PI Controller Using Hybrid Algorithm (GA-PSO) to Reduce Harmonics in Photovoltaic Systems by (Q-ZSI)

Saeed Aslani, Seyed Mohammadjavad Rastegarfatemi*, Alireza Solat

(Department of Electrical Engineering, College of Electrical Engineering and Computer, Saveh Branch, Islamic Azad University, Saveh, Iran)

* Corresponding author: Rastegar.Fatemi@iau.ac.ir

Article History:

Received: September 13, 2024
Revised: October 12, 2024
Accepted: October 21, 2024
Published: November 30, 2024

Abstract: Connecting solar arrays to the main power grid requires an inverter to convert direct current into alternating current. Traditional inverters use electronic devices to convert electricity, which causes time-consuming switching operations and total harmonic distortion (THD) at the inverter output, and ultimately disrupts the power quality in photovoltaic systems. Considering the aforementioned disadvantages of the inverter, in this study, a quasi-impedance source inverter (Q-ZSI) with shoot-through capability was used for power conversion. The latest solution to reduce three-phase inverter losses in this study is the accurate selection of proportional integral (PI) controller parameters using genetic algorithm-particle swarm optimization (GA-PSO), which has been able to improve pulse width modulation (PWM) signals and ultimately reduce harmonics at the output by reducing the overall operating time and appropriate switching in three-phase inverter bridges. The aim of this study is to reduce the losses on the direct-current (DC) side of the inverter. Before connecting the power received from the photovoltaic system to the main grid, the control system operates in a manner that reduces the non-linear loads that cause disturbances and reactive power generation in the grid (AC). The proposed structure is more effective than fuzzy methods and various filtering methods for suppressing harmonics in the inverter, and can create a stable

power grid. The results obtained were presented using the MATLAB/Simulink software.

Keywords: photovoltaic system; hybrid algorithm; total harmonic distortion; quasi-impedance source inverter; proportional integral controller; pulse width modulation

使用混合算法(GA-PSO)优化PI控制器以减少光伏系统中的谐波(Q-ZSI)

摘要：将太阳能电池阵列连接到主电网需要逆变器将直流电转换为交流电。传统逆变器使用电子设备转换电能，这会导致耗时的切换操作和逆变器输出的总谐波失真(THD)，并最终破坏光伏系统的电能质量。考虑到逆变器的上述缺点，在本研究中，使用具有直通能力的准阻抗源逆变器(Q-ZSI)进行功率转换。本研究中减少三相逆变器损耗的最新解决方案是使用遗传算法-粒子群优化(GA-PSO)精确选择比例积分(PI)控制器参数，它能够改善脉冲宽度调制(PWM)信号，并通过减少总运行时间和适当切换三相逆变桥来最终减少输出谐波。本研究的目的是减少逆变器直流(DC)侧的损耗。在将光伏系统接收到的电力连接到主电网之前，控制系统以减少引起电网(AC)干扰和无功功率产生的非线性负载的方式运行。所提出的结构比模糊方法和各种滤波方法更有效地抑制逆变器中的谐波，并且可以创建稳定的电网。使用MATLAB/Simulink软件展示了获得的结果。

关键词：光伏系统; 混合算法; 总谐波失真; 准阻抗源逆变器; 比例积分控制器; 脉冲宽度调制

1. Introduction

The amount of radiant energy of the sun on Earth is several times the total annual energy consumption on Earth, which shows that these resources are of great importance in meeting the needs of life. Due to the energy crisis, many countries with the advancement of technology are trying to make maximum use of this energy source by replacing photovoltaic systems in electricity production and forget the use of fossil fuels in electricity production. Photovoltaic systems have different power ranges that are used in homes, industries, pumps, etc. The use of PV systems has been increasingly investigated owing to their widespread application in electricity supply. In photovoltaic systems, an inverter connected to the grid is used for power conversion, which is located between the main source and the power grid. It is suitable for converting direct current into alternating current from high-frequency inverters. Low-frequency inverters reduce the power factor, inject non-linear loads into the network, and reduce the quality of voltage and current at the output of the system [1]. Power quality is used to achieve a stable and regular network, which is always discussed in power networks [2-6]. In a power network, to improve power efficiency, the nominal frequency should not be far from the sinusoidal shape in order to reduce losses [7]. In photovoltaic systems, problems that increase losses and decrease energy disturb the power factor of the network, including non-linear loads and voltage fluctuations. For this reason, many researchers have been looking for solutions to solve this problem in recent years [8-13]. Therefore, any disturbance in the mentioned parameters will reduce the power factor of the network and increase system losses. According to the factors of power quality in photovoltaic systems [14], the important topic of this article is harmonic reduction. Traditional inverters use electronic converters to increase the output voltage. In the presence of electronic components for voltage conversion, a significant amount of time is lost during the switching operation. Therefore, THD is created at the output of the inverter. Finally, harmonic distortion appears, and in general, the existence of harmonics in photovoltaic systems can be defined as a specific disorder [15-19].

A comprehensive review of harmonics in photovoltaic systems is presented. According to the obtained results, the total harmonic distortion in photovoltaic systems was investigated in different scenarios. Non-linear loads in small and also large networks of photovoltaic systems have different harmonics compared to the distance of the equipment used; harmonics increase and cause the ideal current and voltage to not be created in the network [20]. In addition, the impedance of the photovoltaic system and the connection point to the main grid affect the output harmonics [21]. According to a review of past works, in most studies, there is a gap in the new evolving methods for improving the power factor at the inverter output. Therefore, to fill this research gap, in this study, a new solution is proposed to eliminate inverter switching losses. According to the innovation in this

study with the aim of reducing harmonics in photovoltaic systems, using the GA-PSO algorithm and optimizing the pulse width modulation (PWM) signals through the control system and creating suitable pulses for inverter IGBTs reduces losses in inverter switching. According to [28], which presented the harmonics in the (Q-ZSI) in the fuzzy algorithm mode, in this study, using the hybrid algorithm (GA-PSO) and optimizing the values of the proportional-integral controller (PI) reduced the harmonics and had a significant impact on the power quality of the main network.

The remainder of this paper is organized as follows: In Section 2, the construction of a quasi-impedance source inverter (Q-ZSI) with shoot-through features is presented. Section 3 describes the structure of the system. In Section 4, the simulation results are presented in detail, and in Section 5, general results are presented.

2. QZS Inverter

Impedance inverters can be very effective in power conversion owing to their structure. The structure of this topology is placed between the main voltage sources, and the load shown in Figure 1 has two inductors and two capacitors. This structure has several advantages, including reducing and increasing the voltage and balancing the capacitor voltage [22-24]. According to the aforementioned advantages, this structure also has disadvantages, which is why it has been investigated in many centers. The inverter (Z) has disadvantages compared to the unique quasi-impedance (QZ) structure; thus, the advantages of the quasi-impedance (QZ) inverter are currently used in the power grid [25, 26]. The structure of the inverter includes a DC filter capacity C, inductance L1-L2, energy storage capacity C1-C2 and diode D1. The structure (QZ) is shown in Figure 1.

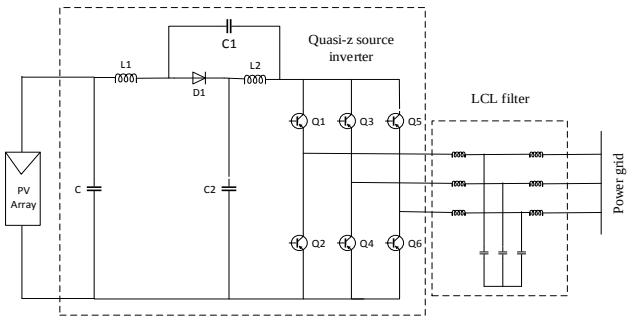

Figure 1. Structure of QZSI (authors' design)

The impedance structure has shoot-through and non-shoot-through (active) modes, which significantly affect switching. The switching modes are listed in Table 1.

Table 1. Switching modes (compiled by the authors)

Switching state	S_1	S_4	S_3	S_6	S_5	S_2
Active state (1 0 0)	1	0	0	1	0	1
Active state (1 1 0)	1	0	1	0	0	1
Active state (0 1 0)	0	1	1	0	0	1
Active state (0 1 1)	0	1	1	0	1	0
Active state (0 0 1)	0	1	0	1	1	0
Active state (1 0 1)	1	0	0	1	1	0
Null state (0 0 0)	0	1	0	1	0	1
Null state (1 1 1)	1	0	1	0	1	0
Shoot through state	1	1	ϕ	ϕ	ϕ	ϕ
Shoot through state	ϕ	ϕ	1	1	ϕ	ϕ
Shoot through state	ϕ	ϕ	ϕ	ϕ	1	1
Shoot through state	1	1	1	1	ϕ	ϕ
Shoot through state	1	1	ϕ	ϕ	1	1
Shoot through state	ϕ	ϕ	1	1	1	1
Shoot through state	1	1	1	1	1	1

2.1 Description of Switching Modes in (QZSI)

The equivalent circuit in the three modes with different performances is shown in Figure 2.

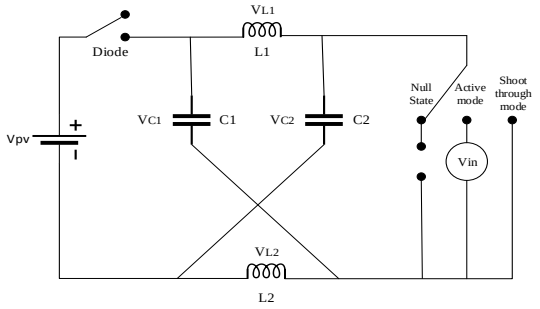

Figure 2. The (Q-ZSI) equivalent circuit (authors' design)

2.1.1 Null Mode

In this mode, as shown in Figure 1, the upper and lower legs are short-circuited and the circuit is open. The three-state circuit is illustrated in Figure 2.

2.1.2 Shoot through Mode

Based on the 15 switching modes of the inverter, this section includes seven short-circuit modes that direct the generated energy to the inverter output. In this case, the switches can be turned off and on at the same time, but in traditional inverters, connecting the switches in one base causes loss of the main source. Owing to the equality of the inductors and capacitors, the impedance network becomes symmetrical, and its equivalent circuit is obtained as follows:

$$V_{c1} = V_{c2} = V_c \quad V_{L1} = V_{L2} = V_L \tag{1}$$

The equivalent circuit of the qZSI during the shoot-through is shown in Figure 3.

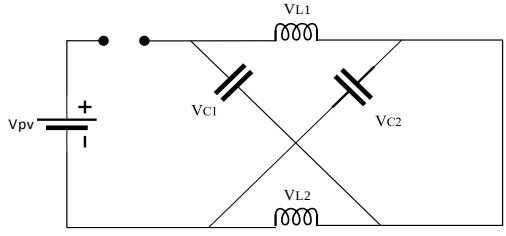

Figure 3. Shoot through circuit (authors' design)

During the shoot through time, it is obtained:

$$V_L = V_C \quad V_o = 0 \tag{2}$$

2.1.3 Non-Shoot through Mode (Active)

In this mode, it works like a traditional inverter in that the inductor current is reduced, and the energy is not transferred to the output of the inverter. According to table (1), there are six active modes where the up or down keys are active, and they cannot connect two opposite pins simultaneously. The circuit is illustrated in Figure 4.

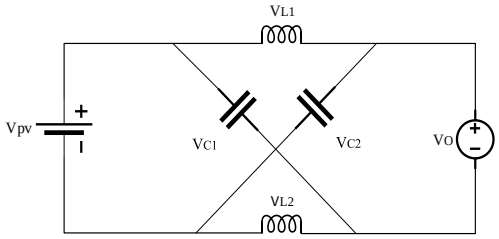

Figure 4. Non-shoot through circuit (authors' design)

During non-shoot through time, we get:

$$V_o = V_C - V_L = 2V_C - V_{pv} \quad V_L = V_{pv} - V_C \tag{3}$$

The capacitor voltage can be obtained:

$$\frac{T_{nsh}}{T_{nsh}-T_{sh}} V_{pv} = \frac{1-D}{1-2D} V_{pv} \tag{4}$$

where T = Tnsh + Tsh is the amount of switching time in the inverter and D is the function of the launch time during operation in the inverter, Vpv is the input voltage and VC is the capacitor voltage, because:

$$V_L = V_C$$

$$V_o = \frac{1-D}{1-2D} V_{pv} \tag{5}$$

$$M = 1 - D \text{ or } D = 1 - M \tag{6}$$

According to Equation 6, coefficient B can be obtained as follows:

$$B = \frac{1}{1-2D} \geq 1 \tag{7}$$

As results from Equations 6 and 7,

$$B = \frac{1}{2M-1} \tag{8}$$

3. Proposed Method

According to Figure 6, the PV system receives solar energy using the control system to absorb the maximum power point tracking (MPPT) before entering the inverter [27]. A quasi-impedance source inverter (Q-ZSI) with a shoot-through feature was used for power conversion. According to [28], which uses a fuzzy control system (Figure 5) to reduce the harmonics in the output of the inverter, in this study, the hybrid algorithm (GA-PSO) was used to optimize the parameters of the PI controller and reduce the THD of the inverter.

3.1. PV Array

Solar cells are used to absorb energy in photovoltaic systems, which consist of a number of small PV cells with different specifications. The cell circuit is shown in Figure 5.

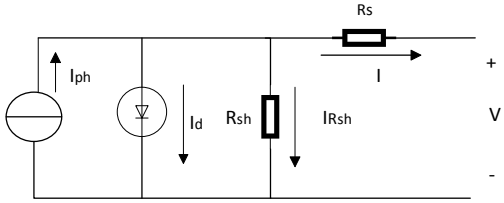

Figure 5. PV cell equivalent circuit (authors' design)

PV output current is obtained:

$$I = I_{ph} - I_d \left\{ exp\left[\frac{q(V + R_s I)}{nKT}\right] - 1 \right\} - \frac{V + R_s I}{Rsh} \tag{9}$$

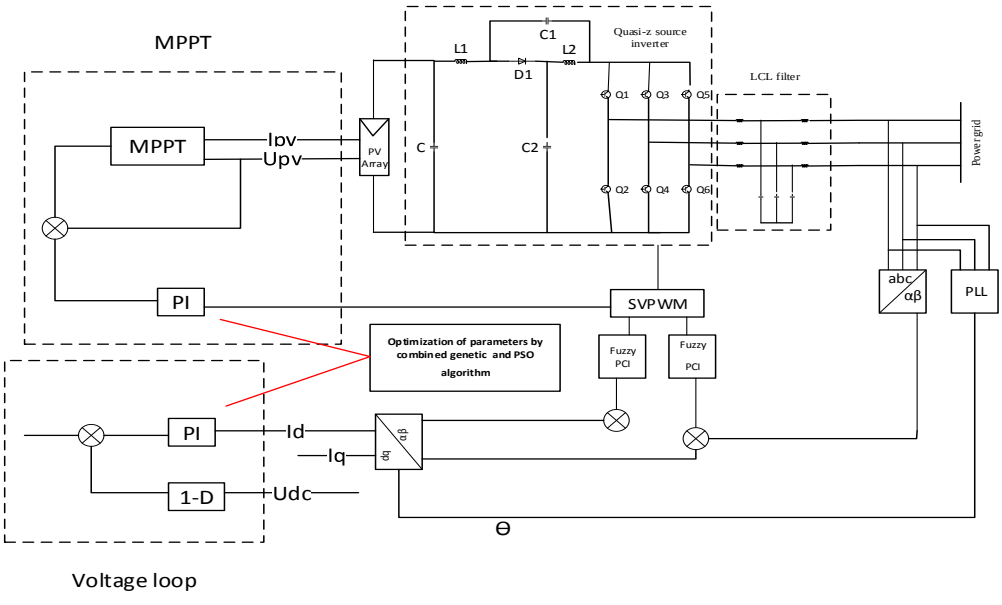

Figure 6. General structure of the system (authors' design)

In Figures 5 and 6, *I* is the current of the photovoltaic cell. The light produced by the panels was *Iph*. The network series resistance is *Rs*. The network shunt resistance is denoted as *Rsh*. The parallel current resistance is denoted by *IRsh*. The output voltage of the PV cells is known as *V*, where *Q* is the charge of the electron. The Boltzmann constant is denoted as *K*. The temperature received from the PV panel is denoted as *T*.

3.2.1. Genetic Algorithm

The genetic algorithm is a search and optimization method based on the principles and mechanisms of natural genetics and the selection of survival of the fittest. Basic concepts in genetic algorithm and its types of operators

● Chromosome: A group of bits used to represent each member of a set.

● Coding: The manner in which chromosomes are displayed is called chromosome coding.

● Population: Set of chromosomes.

● Intersection operator: This operator operates on a pair of chromosomes, and the two chromosomes are randomly broken from a point and move parts of two chromosomes. In this way, two new chromosomes are obtained.

● Mutation: In this step, a random chromosome is selected from the population. By changing this, a new chromosome is randomly created. A flowchart of the algorithm (GA) is shown in Figure 7.

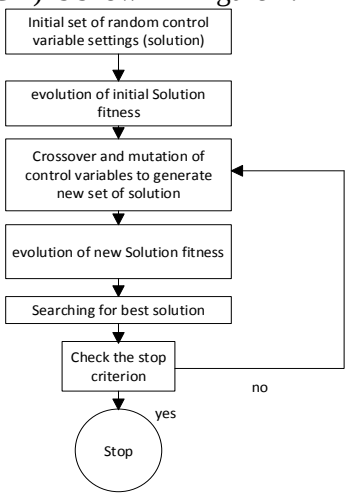

Figure 7. Flowchart of the genetic algorithm (authors' design)

3.2.2. Particle Swarming Algorithm

In the PSO algorithm, the acceptable position and velocity of the particles were randomly determined. The position and velocity of the *i*-th particle in step are as follows:

$V_{L1} = V_{i1}(t).V_{i2}(t).\ldots.V_{iD}(t)\ \&\ X_i(t) = V_{i1}(t).V_{i2}(t).\ldots.V_{iD}(t)\ \&\ X_{id}(t) \epsilon [\, l_d\,.\, u_d\,.\,(t)]$, $d \epsilon$ [1,D] (10)

The position and velocity vectors of the particles were updated according to the following relations:

$V_{ij}(t+1)\ \omega V_{ij}(t) + c_1 r_{1ij}\big[\, p_{ij}(t) - x_{ij}(t)\big] + c_2 r_{2ij}\,[g_i(t) - x_{ij}(t)]$

$x_{ij}(t+1) = x_{ij}(t) + v_{ij}(t+1)$ (11)

where ω is the inertial weight, and $r_{1ij}$and $r_{2ij}$are two separate random numbers with a uniform distribution [0,1]. The velocity coefficients c_1 - c_2 are two constant positive numbers, and t is the number of iterations of the algorithm. The best previous position that the *i*-th particle has experienced thus far is denoted by $p_{besti}(t) = p_{i1}(t)\,.p_{i2}(t)\ldots.p_{iD}(t)$ shows and the best personal experience is called the *i*-particle.

The steps of the PSO method can be described as follows:

Suppose t=0, randomly create an initial population with swarm *M* and corresponding speeds, for each *i* put 1<i<M, $p_{besti}(0) = x_i(0)$, and then the value of $G_{best}(0)$ is calculated using the following equation:

$G_{best}(0) = arg_{xi(0)\,.1<i<m}\min\ f((x_i(0))$ (12)

According to (13), for each *i*, 1<i<M, compare the value of the particle's objective function with the value of the objective function. If the value of the particle's function is lower than the value of the objective function, it is placed as the best particle *i* in step t+1; otherwise, this form is the best particle *i* at time t+1 of the test experience of particle *i*, which is in stage t.

$p_{besti}(t+1) = X_i(t+1).\ and\ otherwise$

$f\ X_i(t+1) < f\ ((p_{besti}(t)\ \&\ X_i(t+1)\ \epsilon\ s$ (13)

According to (14), at step t+1, select the best particle that has the lowest value of the objective function among the best particle experiences.

$G_{best}(t+1) = arg_{p_{besti}\,.1<i<m}\min f\,(p_{besti}(t+1)$ (14)

The flowchart of the algorithm (PSO) is given in Figure 8.

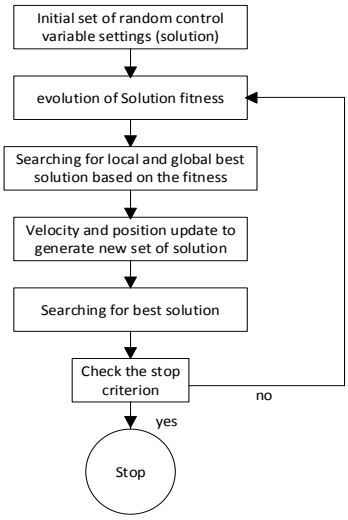

Figure 8. Flowchart of particle swarm optimization algorithm (authors' design)

3.2.3. Hybrid Algorithm (GA-PSO)

The hybrid algorithm is a computer control and optimization method that has been used. Hybrid algorithms solve the same problem but have different features and performance, which are combined to provide the final goal. A flowchart of the algorithm (GA-PSO) is shown in Figure 9.

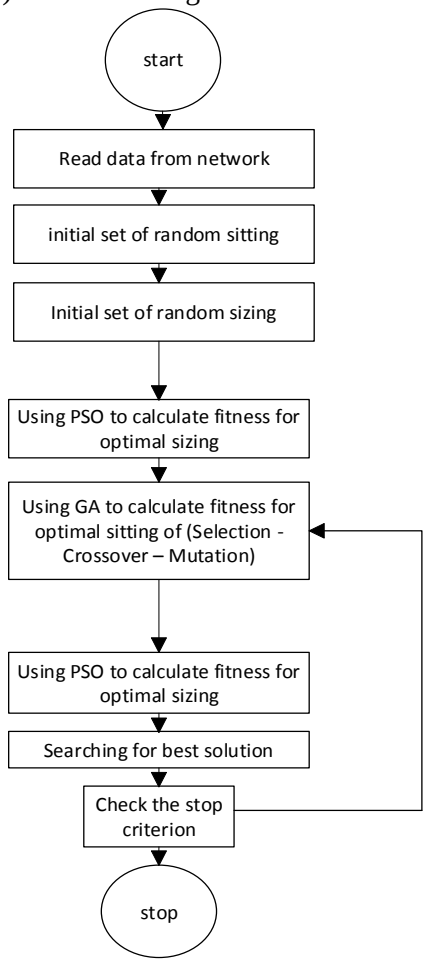

Figure 9. Flowchart of hybrid Algorithm (GA-PSO) (authors' design)

3.3. Objective Function

The following functions are used to minimize the THD at the inverter output: where f1, f2, and f3 are defined as follows:

$$\min_{u.w \in z} f_1 = THD_i\,(x.u.w) \quad (15)$$

$$\min_{u.w \in z} f_2 = max_{i \in \Omega_l} THD_{v.i}\,(x.u.w) \quad (16)$$

$$\min_{w \in z} f_3 = \sum(d_i + s_{ci}q_{ci} + s_{ri}q_{ri})_{i \in \Omega} \quad (17)$$

subject to:

$$L(x, u, w) = 0 \quad (18)$$

$$G(x, u, w) \leq 0 \quad (19)$$

In the up function, the state variable is denoted by *x*. The control variable is specified by *u*, the new variable in the harmonic filters is indicated by *w*, and Ω denotes the harmonic filter in the function. The cost of the harmonic filter function is denoted by *d*. The costs of the reactor unit and capacitor were s_{ri} و s_{ci}. Capacitive and inductive compensations in the function are indicated by q_{ci} و q_{ri}, respectively, which are added to the harmonic filter. The distortion of the total harmonic current in the function is characterized by THD_i, which has a common point. The total harmonic voltage distortion in the function is denoted by $THD_{v.i}$, which is on bus *i*. The equality and inequality constraints are denoted as *L* and *G*, respectively.

3.4. Suggested Inverter Controller

A control system (PI) with suitable features can be used with smart algorithms for optimal solutions in the electrical sciences. *Kp* and *Ki* are the control parameters of PI. The purpose of this method is to optimally adjust the parameters of *Kp* and *Ki* coefficients of the PI controller, and by using the hybrid algorithm (GA-PSO), the optimal coefficients can be adopted in such a way that the objective function reaches its minimum value. The range of values of the PI controller parameters was considered to be 0 < Ki < 1100 and 0 < Kp < 1 for optimization. The ideal values were Ki=337.18 and Kp=0.91.

In the PI-based control technique, the PWM signals generated in the QZSI inverter are used for the optimal switching of the inverter, which reduces the losses in the switching operation of the inverter. A block diagram of the control system is shown in Figure 10.

4. Simulation

In this section, the results obtained using the Simulink software are presented. The system parameters are presented in Table 2. In this study, a network-connected control system model based on PI control is presented based on system simulation results.

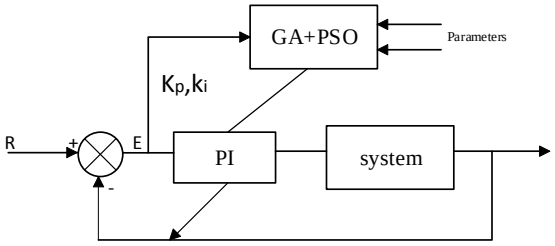

Figure 10. System control block diagram (authors' design)

Table 2. System parameters (compiled by the authors)

Parameters system	value
Grid voltage / V	380
Line frequency / Hz	50
Switching frequency / Hz	1*104
Filter inductance /mH	3
Filter capacitance / μF	2
DC filter capacitance /μF	2000
Impedance source network capacitance	570
Impedance source network inductance	1000

The parameters and values of the photovoltaic system are presented in Table 3. By connecting the modules in series, it shows the voltage stability in the PV system, and by connecting the modules in parallel, it shows the reliability of the current in the PV system. In this study, ten series modules and two parallel modules were used in the PV system.

Table 3. PV parameters (compiled by the authors)

Parameters PV	Value
Voltage / V	37.6
Current /A	7.45
Maximum power point voltage/ V	31
Maximum power point current/A	8
Number of serial modules	10
Number of parallel modules	2

The waveforms of the signals generated before the impedance inverter are shown in Figure 11. By comparing the shoot-through lines with triangular waves, where the triangular shape is larger than the sinusoidal shape, the inverter switches are connected. If the opposite is true, the inverter switch is off. The switching action of the switch creates a sinusoidal circuit at the inverter output.

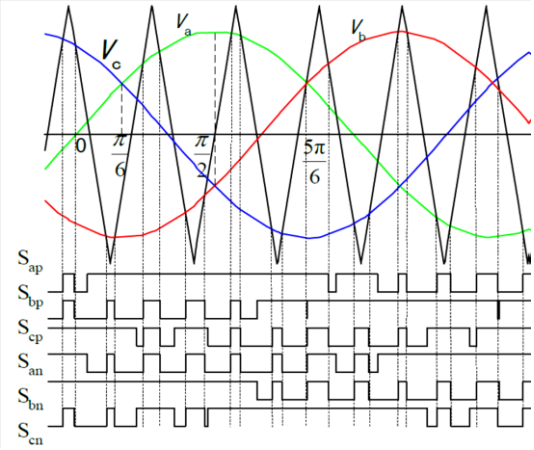

Figure 11. Q-ZSI output pulses (developed by the authors)

According to mathematical calculations, taking each of the switching functions as a Fourier series expansion relationship, the voltages Vao, Vbo, and Vco in the general state are as follows:

$$Vao = \frac{vd}{2}Sa = \frac{vd}{2}\sum_{n=1}^{\infty} A_n sin\,(n\omega t) \quad (20)$$

$$Vbo = \frac{vd}{2}Sb = \frac{vd}{2}\sum_{n=1}^{\infty} A_n sin\,(n\omega t - 120) \quad (21)$$

$$Vco = \frac{vd}{2}Sc = \frac{vd}{2}\sum_{n=1}^{\infty} A_n sin\,(n\omega t - 240) \quad (22)$$

Using the above relationships, the line voltages of the inverters are obtained as follows:

$$Vab = Vao - Vbo = \frac{\sqrt{3}}{2}Vd\sum_{n=1}^{\infty} A_n sin\,n(\omega t + 30) \quad (23)$$

$$Vbc = Vbo - Vco = \frac{\sqrt{3}}{2}Vd\sum_{n=1}^{\infty} A_n sin\,n(\omega t - 90) \quad (24)$$

$$Vca = Vco - Vao = \frac{\sqrt{3}}{2}Vd\sum_{n=1}^{\infty} A_n \sin(n\omega t + 150) \quad (25)$$

To calculate the phase voltages, we act as follows:

$$Vno = \frac{1}{3}\,Vao = Vbo - Vco \quad (26)$$

$$Van = Vao - Vno \quad (27)$$

$$Vbn = Vbo - Vno \quad (28)$$

$$Vcn = Vco - Vno \quad (29)$$

The output current and voltage of the inverter on the AC side are shown in Figures 12 and 13. The array was exposed to solar radiation with balanced light of 1000 W and a temperature of 25°C. The output voltage was 380 volts and the output current was 8 A.

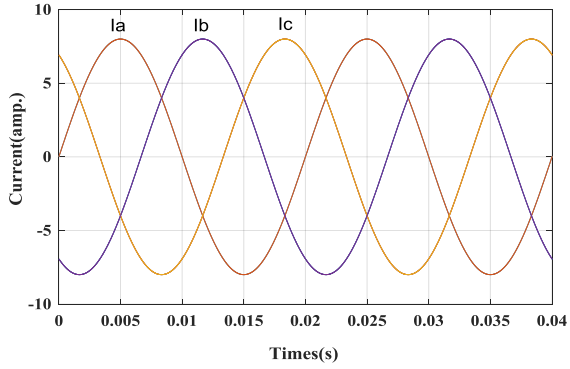

Figure 12. Inverter output current (developed by the authors)

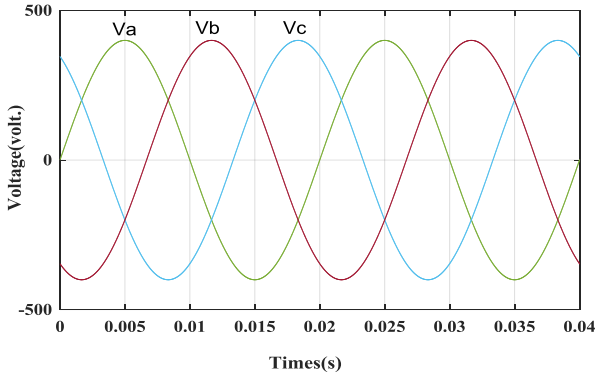

Figure 13. Inverter output voltage (developed by the authors)

The following figures show the current–voltage output curves. First, when the panels are in the circuit, there is an overshoot in voltage and current. According to Figure 14, the voltage curve is damped after 0.2 seconds and reaches its stable state with the value of 380 volts. The starting current decays in 0.3 seconds and finally reaches a steady state with a current of 8 A, as shown in Figure 15.

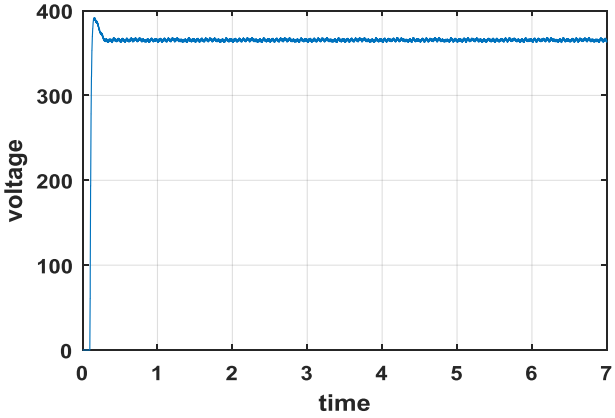

Figure 14. Voltage output curve (developed by the authors)

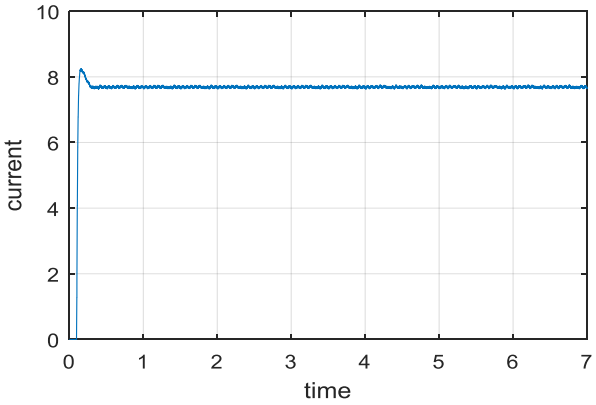

Figure 15. Current output curve (developed by the authors)

The important topic of this study is the reduction of three-phase inverter output harmonics in photovoltaic systems. As shown below, the simulation results of the harmonics in the three controllers were recorded and compared according to the results. According to [28], which reduces the harmonics with the fuzzy control system, in this study, a hybrid algorithm (GA-PSO) is used to optimize the parameters of the PI controller. In addition, for DC/AC conversion, a quasi-impedance source inverter (Q-ZSI) with shoot-through capability was used to improve the switching performance.

The harmonic results are shown in Figures 16, 17 and 18.

The output THD of the inverter in the hybrid, FUZZY, and PI controllers were recorded as 3.81, 5.88, and 8.94, respectively. The results show that using the hybrid algorithm (GA-PSO) reduces THD and does not introduce non-linear loads into the main network. Meanwhile, it has been confirmed that the hybrid algorithm control system is superior to the fuzzy system in suppressing harmonics in photovoltaic systems.

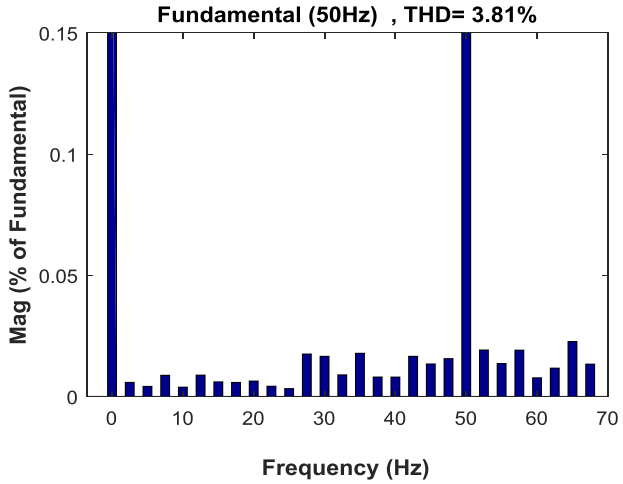

Figure 16. Harmonic output with PI controller (developed by the authors)

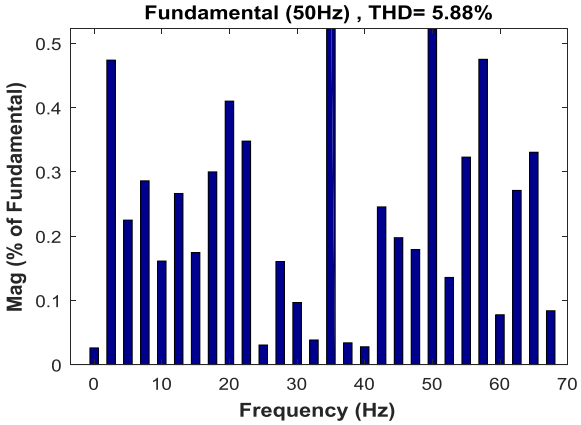

Figure 17. Harmonic output with PI controller (developed by the authors)

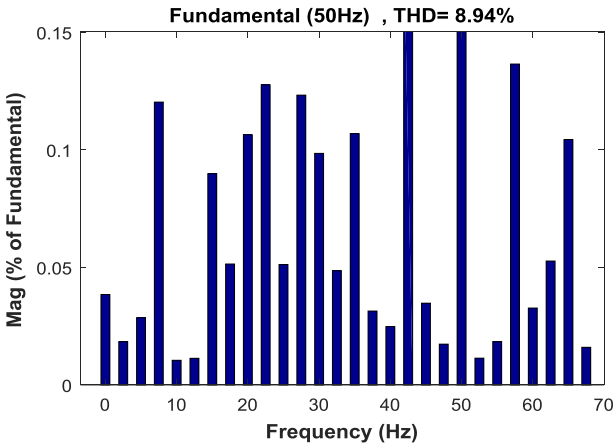

Figure 18. Harmonic output with PI controller (developed by the authors)

The steady error of the network in the three

methods: PI controller, fuzzy, and hybrid algorithm (GA-PSO) is shown in Figure 19. In the PI controller, the steady error decreased as the current increased. According to the results, the error in the steady state and the AC signal cannot be eliminated using the PI controller. In the fuzzy method, the steady error of the system was better and more stable than that of the PI method. In comparison, the hybrid algorithm control method was significantly superior to the PI and fuzzy methods in terms of steady error control.

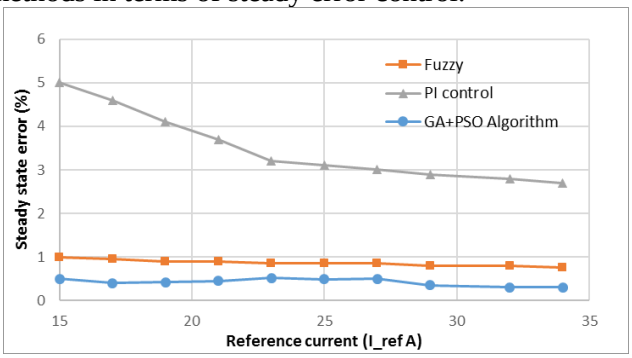

Figure 19. The steady error in 3 methods (developed by the authors)

5. Discussion

The main factors of power-quality disturbance include harmonic distortion, frequency fluctuations, and voltage imbalance, all of which need to be controlled and investigated. This study examines the harmonics in three-phase photovoltaic systems. In traditional inverters, owing to the dead time for switching between two switches facing each other, it is one of the most important weaknesses and produces harmonics. The most important factor in increasing losses is switching in the inverter for power conversion; therefore, in this study, a suitable inverter (Q-ZSI) is used for switching and power transmission, as well as the latest method and mastery of the control system that has the problem. It reduces harmonics and compares and is superior to the most up-to-date methods. According to a comprehensive study on harmonic distortion systems in photovoltaic systems, the location and number of equipment associated with harmonic generation, outages, inverters, transformers, generators, as well as at the common points (PCC) between the output of the photovoltaic system and the main power grid, causes harmonic distortion. According to this research and comprehensive study on harmonics, it is possible to propose methods to reduce harmonics in photovoltaic systems, select the exact number of inverters, and select the appropriate location of generators, transformers, and local loads. Modern control methods improve the power quality of grids.

6. Conclusion

In a photovoltaic system, an inverter connected to the grid is used for power conversion (DC/AC), which is located between the main source and the power grid. In this study, a three-phase quasi-impedance source inverter (Q-ZSI) with shoot-through capability was used to convert and transmit power in a photovoltaic system. Considering the main focus of the reduction of harmonics, in this study, by using the hybrid algorithm GA-PSO, we have been able to adjust the PI control parameters in such a way that the PWM signals are optimized, and by making ideal pulses for IGBT inverter, the harmonics on the AC side of the inverter are reduced and compared with the fuzzy control system. In comparison, the use of the hybrid algorithm GA-PSO reduces the number of generated harmonics (non-linear loads) and then reduces the losses when connected to the main power grid. According to the obtained results, the hybrid algorithm is superior to the fuzzy system in suppressing the harmonics. Simulation results in MATLAB/Simulink software have proven the ability of new structures in photovoltaic systems to reduce harmonics.

Recommendation on the work done and its perspective:

Considering the conduct of this research, which is about (THD) in photovoltaic systems, it is recommended to use different combined algorithm methods and comparative modes with each other, as well as using modern control systems to optimize parameters and ultimately achieve better power factor and stability of the power grid. Thus, engineers in this field can have a bright future using clean energy from an open perspective.

Declarations

Author Contributions

Conceptualization, S.M.R. and A.S.; methodology, S.A., S.M.R. and A.S.; software, S.A. and A.S.; formal analysis, S.A.; investigation, S.A., S.M.R. and A.S.; resources, S.A., S.M.R. and A.S.; data curation, S.M.R.; writing—original draft preparation, all authors contributed equally; writing—review and editing, S.A.; visualization, S.A.; supervision, S.M.R. and A.S.; project administration, S.M.R. All authors have read and agreed to the published version of the manuscript.

Data Availability Statement

The data presented in this study are available on request from the corresponding author.

Funding

Funding information is not available.

Acknowledgements

The researchers are especially grateful to Islamic Azad University, Saveh Branch, for providing all the

opportunities from the beginning to the end of this work.

Conflicts of Interest

The authors declare that there is no conflict of interests regarding the publication of this manuscript. In addition, the ethical issues, including plagiarism, informed consent, misconduct, data fabrication and/or falsification, double publication and/or submission, and redundancies have been completely observed by the authors.

References

[1] ELKHOLY A. Harmonics assessment and mathematical modeling of power quality parameters for low voltage grid connected photovoltaic systems. *Solar Energy*, 2019, 183: 315–326.

[2] MAHELA O, SHAIK A, GUPTA N, KHOSRAVY M, KHAN B, HAES ALHELOU H, & PADMANABAN S. Recognition of Power Quality Issues Associated With Grid Integrated Solar Photovoltaic Plant in Experimental Framework. *IEEE Systems Journal*, 2020, 15(3): 3740–3748. https://doi.org/10.1109/JSYST.2020.3027203

[3] BABU N P, GUERRERO J M, SIANO P, PEESAPATI, R. & PANDA G. A Novel Modified Control Scheme in Grid-Tied Photovoltaic System for Power Quality Enhancement. *IEEE Transactions on Industrial Electronics*, 2021, 68: 11100–11110. https://doi.org/10.1109/TIE.2020.3031529

[4] ZHANG X P, & YAN Z. Energy Quality: A Definition. *IEEE Open Access Journal of Power Energy*, 2020, 7, 430–440.

[5] JAYARAJU G. & RAO G S. Intelligent controller based power quality improvement of microgrid integration of photovoltaic power system using new cascade multilevel inverter. *International Journal of Electrical and Computer Engineering*, 2019, 9(3): 1514–1523. http://doi.org/10.11591/ijece.v9i3.pp1514-1523

[6] MOGHASSEMI A, HOSSEINI M, & OLAMAEI J. Power Quality Improvement of Grid-Connected Photovoltaic Systems Using Trans-Z-Source Inverter Under Partial Shading Condition. *Iranian Journal of Science and Technology Transactions of Electrical Engineering*, 2020, 44, 1429–1447. http://doi.org/10.1007/s40998-020-00338-0

[7] YU S, ZHANG L, IU H H C, FERNANDO T, & WONG K P. A DSE-Based Power System Frequency Restoration Strategy for PV-Integrated Power Systems Considering Solar Irradiance Variations. *IEEE Transactions on Industrial Informatics*, 2017, 13: 2511–2518.

[8] ADIANANDA, KISWANTONO A, and AMIRULLAH. Multi units of three phase photovoltaic using band pass filter to enhance power quality in distribution network under variable temperature and solar irradiance level. *International Journal of Electrical and Computer Engineering*, 2018, 8(2): 806–817, http://doi.org/10.11591/ijece.v8i2.pp806-817.

[9] ORTEGA M J, HERNÁNDEZ J C, & GARCÍA O G. Measurement and assessment of power quality characteristics for photovoltaic systems: Harmonics, flicker, unbalance, and slow voltage variations. *Electric Power Systems Research*, 2013, 96: 23–35. https://doi.org/10.1016/j.epsr.2012.11.003

[10] OMRAN W A, KAZERANI M, and SALAMA M M A. Investigation of methods for reduction of power fluctuations generated from large grid-connected photovoltaic systems. *IEEE Transactions on Energy Conversion*, 2011, 26(1): 318–327, http://doi.org/10.1109/TEC.2010.2062515.

[11] KSENTINI A, HADEF Z, AZZAG E B, NECAIBIA S, & NECAIBIA, A. Technico and economic optimization of the injection of a photovoltaic system on a low voltage network. *The Scientific Bulletin of Electrical Engineering Faculty*, 2023, 23(1): 1-8, Valahia University of Targoviste, http://doi.org/10.2478/sbeef-2023-0001.

[12] JAYACHANDRAN J, & MALATHI S. Improved power quality buck boost converter for SMPS. *International Journal of Electrical and Computer Engineering*, 2019, 9: 789.

[13] REZVANI F, MOZAFARI B, & FAGHIHI F. Power quality analysis for Photovoltaic system considering unbalanced voltage. *Indian Journal of Science and Technology*, 2015, 8(14): 1-7. http://doi.org/10.17485/ijst/2015/v8i14/60194

[14] GRYCAN W, BRUSILOWICZ B. & KUPAJ M. Photovoltaic farm impact on parameters of power quality and the current legislation. *Solar Energy*, 2018, 165: 189–198.

[15] RAHMOUNI W, BACHIR G, and AILLERIE M. PAPERS A new control strategy for harmonic reduction in photovoltaic inverters inspired by the autonomous nervous system. *Journal of Electrical Engineering*, 2022, 73: 310–317. http://doi.org/10.2478/jee-2022-0041

[16] FAN Y, ZHOU Q, WANG J, MU S. & WANG L N. Application of Superconducting-Magnetic-Energy-Storage-Based Current-Source Active Power Filter in Photovoltaics for Harmonic Mitigation. *IEEE Transactions on Applied Superconductivity*, 2021, 31(8): 8–11. https://doi.org/10.1109/TASC.2021.3088766

[17] MAAROUF S, KSENTINI A, and AZZAG E L B. Comparative Study of Five Mppt Controls in Two-Stage Three-Phase Grid-Connected Photovoltaic Systems Under Partial Shading Conditions. *The Scientific Bulletin of Electrical Engineering Faculty*, 2023, 23: 21–30, http://doi.org/10.2478/sbeef-2023-0004.

[18] TADJER S A, HABI I, NADJI B. & KHELIFI F. Harmonics compensation system based on photovoltaic generator. *International Symposium on Power Electronics Power Electronics, Electrical Drives, Automation and Motion*, Sorrento, Italy, 2012, pp. 1119-1122, http://doi.org/10.1109/SPEEDAM.2012.6264596.

[19] VINAYAGAM A, AZIZ A, BALASUBRAMANIYAM P M, J. CHANDRAN J, VEERASAMY V, and GARGOOM A. Harmonics assessment and mitigation in a photovoltaic integrated network. *Sustainable Energy, Grids and Networks*, 2019, 20: 100264, http://doi.org/10.1016/j.segan.2019.100264.

[20] ÇELEBI A, & ÇOLAK M. The effects of harmonics produced by grid connected photovoltaic systems on electrical networks. *ELECO`2005 Proceedings of the 4th International Conference on Electrical and Electronics Engineering Papers.*

[21] DE OLIVEIRA P S, LIMA M A A, CERQUEIRA A S, DUQUE C A, & FERREIRA D D. Harmonic analysis based on scica at PCC of a grid-connected micro solar PV power

plant. *Proceedings of the 18th International Conference on Harmonics and Quality of Power (ICHQP)*, Ljubljana, Slovenia, 2018, 1–6. https://doi.org/10.1109/ICHQP.2018.8378875
[22] MOGHASSEMI A, PADMANABAN S, RAMACHANDARAMURTHY V K, MITOLO M. & BENBOUZID M. A Novel Solar Photovoltaic Fed TransZSI-DVR for Power Quality Improvement of Grid-Connected PV Systems. *IEEE Access*, 2021, 9: 7263–7279.
[23] BETTAHAR F, SABRINA A, & ACHOUR B. Enhancing PV Systems with Intelligent MPPT and Improved control strategy of Z-Source Inverter. *Power Electronics and Drives*, 2024, 9(44): 1–20, http://doi.org/10.2478/pead-2024-0001.
[24] DAVE H B, SINGH D, and BANSAL H O. Multiple linear regression-based impact analysis of impedance network design on life expectancy of DC-link capacitor in q-ZSI fed motor drive. *Engineering Science and Technology, an International Journal*, 2021, 24(1): 171–182, http://doi.org/10.1ournal016/j.jestch.2020.06.004.
[25] AKSHATH N S S, NARESH A, KUMAR M N, BARMAN M, NANDAN D, & ABHILASH T. Analysis and simulation of even-level quasi-Z-source inverter. *International Journal of Electrical and Computer Engineering*, 2022, 12: 3477–3484. http://doi.org/10.11591/ijece.v12i4.pp3477-3484
[26] GE B, LIU Y, ABU-RUB H, BALOG R S, PENG F Z, SUN H, and LI X. An Active Filter Method to Eliminate DC-Side Low-Frequency Power for a Single-Phase Quasi-Z-Source Inverter. *IEEE Transactions on Industrial Electronics*, 2016, 63(8): 4838–4848. https://doi.org/10.1109/TIE.2016.2551680
[27] MAAROUF S, KSENTINI A, AZZAG E L B, and KEBBACHE R. Improved artificial neural network design for Mppt grid-connected photovoltaic systems. *The Scientific Bulletin of Electrical Engineering Faculty*, 2022, 22(2): 26-31, Valahia University of Targoviste, http://doi.org/10.2478/sbeef-2022-0016.
[28] HOU T, ZHANG C Y, and NIU H X. Quasi-Z Source Inverter Control of PV Grid-Connected Based on Fuzzy PCI. *Journal of Electronic Science and Technology*, 2021, 19(3): 274–286, http://doi.org/10.1016/j.jnlest.2020.100021.

参考文:

[1] ELKHOLY A. 低压并网光伏系统的谐波评估和电能质量参数的数学建模。太阳能，2019，183：315-326。
[2] MAHELA O、SHAIK A、GUPTA N、KHOSRAVY M、KHAN B、HAES ALHELOU H 和 PADMANABAN S. 在实验框架中识别与电网集成太阳能光伏电站相关的电能质量问题。IEEE 系统杂志，2020，15(3)：3740-3748。 https://doi.org/10.1109/JSYST.2020.3027203
[3] BABU N P、GUERRERO J M、SIANO P、PEESAPATI、R. 和 PANDA G. 一种用于提高电能质量的并网光伏系统新型改进控制方案。IEEE 工业电子学报，2021，68：11100–11110。https://doi.org/10.1109/TIE.2020.3031529
[4] ZHANG X P 和 YAN Z. 能源质量：定义。IEEE 开放获取电力能源杂志，2020，7，430–440。
[5] JAYARAJU G. 和 RAO G S. 基于智能控制器的光伏电力系统微电网一体化电能质量改进，采用新型级联多电平逆变器。国际电气与计算机工程杂志，2019，9(3)：1514–1523。http://doi.org/10.11591/ijece.v9i3.pp1514-1523
[6] MOGHASSEMI A、HOSSEINI M 和 OLAMAEI J. 部分遮光条件下使用 Trans-Z 源逆变器改善并网光伏系统的电能质量。伊朗科学技术杂志电气工程学报，2020，44，1429–1447。http://doi.org/10.1007/s40998-020-00338-0
[7] YU S, ZHANG L, IU H H C, FERNANDO T, & WONG K P. 考虑太阳辐照度变化的基于 DSE 的光伏集成电力系统频率恢复策略。IEEE 工业信息学学报，2017，13：2511-2518。
[8] ADIANANDA, KISWANTONO A, 和 AMIRULLAH。多组三相光伏机组使用带通滤波器在可变温度和太阳辐照度水平下提高配电网电能质量。国际电气与计算机工程杂志，2018，8(2)：806–817，http://doi.org/10.11591/ijece.v8i2.pp806-817。
[9] ORTEGA M J、HERNÁNDEZ J C 和 GARCÍA O G。光伏系统电能质量特性的测量和评估：谐波、闪烁、不平衡和缓慢的电压变化。电力系统研究，2013，96：23–35。https://doi.org/10.1016/j.epsr.2012.11.003
[10] OMRAN W A、KAZERANI M 和 SALAMA M M A。研究减少大型并网光伏系统产生的功率波动的方法。 IEEE 能源转换学报，2011，26(1)：318–327，http://doi.org/10.1109/TEC.2010.2062515。
[11] KSENTINI A、HADEF Z、AZZAG E B、NECAIBIA S 和 NECAIBIA，A。光伏系统在低压电网中注入的技术和经济优化。电气工程学院科学通讯，2023，23(1)：1-8，瓦拉希亚塔尔戈维斯特大学，http://doi.org/10.2478/sbeef-2023-0001。
[12] JAYACHANDRAN J 和 MALATHI S。用于 SMPS 的改进电能质量降压升压转换器。国际电气与计算机工程杂志，2019，9：789。
[13] REZVANI F、MOZAFARI B 和 FAGHIHI F。考虑不平衡电压的光伏系统电能质量分析。印度科学技术杂志，2015，8(14)：1-7。http://doi.org/10.17485/ijst/2015/v8i14/60194
[14] GRYCAN W、BRUSILOWICZ B. 和 KUPAJ M。光伏发电场对电能质量参数和现行立法的影响。太阳能，2018，165：189-198。
[15] RAHMOUNI W、BACHIR G 和 AILLERIE M。论文一种受自主神经系统启发的光伏逆变器谐波降低新控制策略。电气工程杂志，2022，73：310–317。http://doi.org/10.2478/jee-2022-0041
[16] FAN Y、ZHOU Q、WANG J、MU S. 和 WANG L N。基于超导磁能存储的电流源有源滤波器在光伏谐波抑制中的应用。IEEE 应用超导学报，2021，31(8)：8–11。https://doi.org/10.1109/TASC.2021.3088766
[17] MAAROUF S、KSENTINI A 和 AZZAG E L B。部分遮光条件下两级三相并网光伏系统中五种 Mppt

控制的比较研究。电气工程学院科学公报，2023，23：21-30，http://doi.org/10.2478/sbeef-2023-0004。
[18] TADJER SA、HABI I、NADJI B. 和 KHELIFI F。基于光伏发电机的谐波补偿系统。国际电力电子研讨会电力电子、电气驱动、自动化和运动，意大利索伦托，2012，第 1119-1122 页，http://doi.org/10.1109/SPEEDAM.2012.6264596。
[19] VINAYAGAM A、AZIZ A、BALASUBRAMANIYAM P M、J. CHANDRAN J、VEERASAMY V 和 GARGOOM A。光伏一体化网络中的谐波评估与缓解。可持续能源、电网和网络，2019，20：100264，http://doi.org/10.1016/j.segan.2019.100264。
[20] ÇELEBI A 和 ÇOLAK M。电网连接的光伏系统产生的谐波对电网的影响。ELECO`2005 第四届国际电气和电子工程会议论文集。
[21] DE OLIVEIRA P S、LIMA M A A、CERQUEIRA A S、DUQUE C A 和 FERREIRA D D。基于 SCICA 的电网连接微型太阳能光伏电站 PCC 谐波分析。第 18 届国际谐波和电能质量会议 (ICHQP) 论文集，斯洛文尼亚卢布尔雅那，2018，1-6。https://doi.org/10.1109/ICHQP.2018.8378875
[22] MOGHASSEMI A、PADMANABAN S、RAMACHANDARAMURTHY V K、MITOLO M. 和 BENBOUZID M. 一种用于改善并网光伏系统电能质量的新型太阳能光伏供电 TransZSI-DVR。IEEE使用权，2021，9：7263–7279。
[23] BETTAHAR F、SABRINA A 和 ACHOUR B. 使用智能 MPPT 和改进的 Z 源逆变器控制策略增强光伏系统。电力电子与驱动器，2024，9(44)：1–20，http://doi.org/10.2478/pead-2024-0001。
[24] DAVE H B、SINGH D 和 BANSAL H O。基于多元线性回归的阻抗网络设计对 q-ZSI 供电电机驱动器中直流链电容器预期寿命的影响分析。《工程科学与技术》国际期刊，2021，24(1)：171–182，http://doi.org/10.1ournal016/j.jestch.2020.06.004。
[25] AKSHATH N S S、NARESHA A、KUMAR M N、BARMAN M、NANDAN D 和 ABHILASH T。偶数级准 Z 源逆变器的分析与仿真。《国际电气与计算机工程杂志》，2022，12：3477–3484。http://doi.org/10.11591/ijece.v12i4.pp3477-3484
[26] GE B、LIU Y、ABU-RUB H、BALOG RS、PENG F Z、SUN H 和 LI X。一种用于消除单相准 Z 源逆变器直流侧低频功率的有源滤波器方法。IEEE 工业电子学报，2016，63(8)：4838–4848。https://doi.org/10.1109/TIE.2016.2551680
[27] MAAROUF S、KSENTINI A、AZZAG E L B 和 KEBBACHE R。针对 Mppt 并网光伏系统的改进人工神经网络设计。电气工程学院科学公报，2022，22(2)：26-31，瓦拉希亚特尔戈维斯特大学，http://doi.org/10.2478/sbeef-2022-0016。
[28] HOU T、ZHANG C Y、NIU H X。基于模糊 PCI 的光伏并网准 Z 源逆变器控制。电子科学技术学报，2021，19(3)：274–286，http://doi.org/10.1016/j.jnlest.2020.100021。